Chapter

Finite Difference Solution of Conjugate Heat Transfer in Double Pipe with Trapezoidal Fins

Ghazala Ashraf, Khalid S. Syed and Muhammad Ishaq

Abstract

A conjugate heat transfer problem on the shell side of a finned double pipe heat exchanger is numerically studied by suing finite difference technique. Laminar flow with isothermal boundary conditions is considered in the finned annulus with fully developed flow region to investigate the influence of variations in the fin height, the number of fins and the fluid and wall thermal conductivities on the hydraulic and thermal design of the exchanger. The governing momentum and energy equations have been solved by a finite difference-based numerical algorithm. The improvement in heat transfer rates, the exchanger performance and the optimum configurations are discussed.

Keywords: incompressible, laminar flow, convective heat transfer, finned double pipe, fully developed flow, conjugate heat transfer, isotherms

1. Introduction

The theory of heat transfer is widely used in many fields of engineering industries and also in applied sciences. Heat exchangers are being used in power generation houses and nuclear reactor centres, in order to generate and convert energy for unlimited purposes. The design of the heat exchangers, according to its usage, also is a matter of great importance.

As for boiling, condensing and radiating the fluid and other things, the size of heat transfer equipment is always taken into account. In aerospace, equipment requires the limitation of weights, while in nuclear reactors, a deep study of heat transfer analysis is needed to avoid the unbearable damages [1]. In heating, generally these heat exchangers show the very low rate of heat transfer. The performance of such heat exchanger can be signified by various techniques. Özisik [2] has given a detailed study of augmented fin surfaces which are of great help in enhancement of heat transfer rate. A similar study of heat flow was made by Nasiruddin and Kamran [3], for vortex generation by applying baffles in circular ducts. A study on convective heat transfer with variable fin heights was made by Zeitoun and Hegazy [4], in which a rise in heat transfer rate was observed, with low friction factor. Suryanarayana and Apparao [5] mentioned in his work that one of the criteria for evaluating the performance of a heat exchanger with extended surfaces is the pumping power required for a specified heat duty. He reported that average heat transfer coefficient increases with an increase in the frequency of the number of

fins. Another study for heat transfer was made by using elliptic pin finned tube by Qingling et al. [6]. Adegun et al. [7] proposed a new method to increase the heat transfer rate by using circular pipes making them inclined, with different inclinations. They investigated that heat transfer rate is rapid till 15° inclination and fin height H = 0.2 and increase in fin height is just a waste of material and causes more expenses. But before the last few decades, it was not found by any good mathematical approach. Pagliarini [8] indicated that the idealization of infinite conduction may cause unrealistic approach in the analysis of heat transfer characteristics. So, they proposed the idea of finite conductivity offered by the material used in it.

The transfer of heat between fluid and solid while flowing in any heat exchanger is governed by two different kinds of equations, as transfer of heat in fluid is governed by the elliptical Navier-Stokes equation or by the parabolic boundary layer equation, and the heat transfer inside the body is governed by the elliptical Laplace equation or by the parabolic differential equation [9]. This forms a so-called model of conjugate problem. Conjugate heat transfer problems have been analysed in various geometric configurations. Kumar [10] examined two conjugate problems of heat transfer in the laminar boundary layer at the boundary of a semi-infinite porous medium on the assumption that fluid filters continuously through the porous surface and that the injection velocity varies as $x^{-1/2}$. Barozzi and Pagliarini [11] used finite element method to examine a conjugate problem of a laminar flow in a pipe when the outer wall is being heated uniformly to observe the effects of wall conduction.

Mori et al. [12] investigated the conjugate problem in a circular pipe and observed the conduction effects. In this study, it was proposed that conductivities of the wall and of fluid make remarkable affects in heat transfer properties when thickness of the wall is increased, while thin wall effects on the heat transfer properties are negligible. An analysis on conjugate heat transfer by using three types of boundary conditions, as constant heat flux, constant wall temperature and constant heat transfer coefficients, was made by Sakakibara et al. [13]. They used Duhamel's theorem to calculate the interfacial temperature. They reported that conduction in the wall is inversely proportional to the ratio of conductivities of solid to fluid.

Kettner et al. [14] numerically investigated that the ratio of thermal conductivities of the solid to fluid has no noticeable effect when the fins of the small height are considered. However, this conductivity ratio has a significant effect when the fin height relative to pipe radius is taken more than 0.4. A similar conjugate problem was studied in finned tube, and it was reported that fin efficiency has a great influence on heat flux and heat transfer coefficient by Fiebig et al. [15]. The conjugate heat transfer problem was investigated in different geometries by Nguyen et al. [16]. Nordstorm and Berg [17] investigated the Navier-Stokes equations for modified interface conditions. They have computed conjugate problem with two approaches: one is by using heat equation for the transfer of heat in solid, and the other is transfer of heat by using Navier-Stokes equations.

Sohail and Fakhir [18] gave numerical investigation of double-pipe heat exchanger with circumferential fins in longitudinal to study the effect of fin pitch-to-height (P/H) ratio on heat transfer and fluid flow characteristics at various Reynolds numbers, using water as the working fluid. Systematic analysis is carried out by changing geometric and flow parameters. Geometric parameters include varying the pitch-to-height ratio from 0.55 to 26.4, while for the flow parameters, Reynolds number varied from 200 to 1400.

Syed et al. [19] made numerical simulation of finned double-pipe heat exchanger, where fins are distributed around the outer wall of the inner pipe. By using H1 (constant heat flux) and T1 (constant wall temperature) boundary conditions and one-dimensional fin equation, he concluded that the fin heat loss increases

if we increase the conductivity of fin. Mazhar [20] extended the work of Syed [19] by considering laminar conjugate heat transfer in the thermal entrance region of the finned annulus. In his work, finite difference method (FDM) was used for the simulation of the problem of hydrodynamically fully developed and thermally developing and fully developed flow. The investigation made by him was clearly showing that the entrance region is more affected by the ratio of conductivities and rate of heat transfer rate at entrance is higher than that of the fully developed region.

The methods in the previous discussion are conventional methods for enhancing heat transfer rate. They have their own limitations such as the need of extended surfaces, enhancement in thermal processing equipment sizes and increase in pumping power to acquire the desirable efficiency level.

2. Iterative methods

In this chapter, a numerical algorithm for solving elliptic PDEs involving fluid flow and of heat transfer analysis is described. This algorithm uses multigrid discretization for nested iterations to accelerate the rate of convergence at higher levels with less computation. The well-known successive over-relaxation (SOR) method is used to solve the problem, by giving a fixed value to the relaxation parameter. Problems of steady-state viscous flow and steady temperature can be brought into the category of elliptic PDEs with appropriate boundary conditions. In order to solve these PDEs numerically, a higher order accuracy rate with less computation is more preferred. Moreover, estimation of error helps to ensure the accuracy of the solution.

Iterative methods are widely used in order to solve the difference equations, which are obtained from elliptic PDEs. Among these iterative methods, SOR method is widely used for its fast convergence for a class of large linear systems arising from difference equations. SOR method is a quick solver for a large number of linear equations.

The momentum and energy equations are solved by using the algorithm given in the next section, for the behaviour of fully developed laminar flow through a finned double pipe. A comparative study of literature results and the present work are shown in "Results" section.

2.1 Iterative scheme for Poisson equation

$$\text{A general Poisson equation in two dimensions } \nabla^2 u = f(x,y) \qquad (1)$$

can be approximated by the pictorial relation $\nabla^2 u = \frac{1}{h^2}\begin{Bmatrix} & 1 & \\ 1 & -4 & 1 \\ & 1. & \end{Bmatrix}$

The function $u(x,y)$ can be replaced by the value at the discrete nodes of the region. In order to discretize the function, a square grid with step size h can be helpful. The value of the exact solution function $u(x,y)$ at a point $\mathrm{P}(x_i, y_j)$ is denoted by $u\left(x_i, y_j\right)$, and its approximated value is denoted as $u(i,j)$. For the chosen discretization of the function, the partial differential equations are approximated at the grid points by using the discrete value of the function $u(i,j)$. The first- and second-order partial derivatives are approximated by the difference quotients. For this purpose central difference quotients are used as follows:

$$u_x\left(x_i, y_j\right) = \frac{u_{i+1,j} - u_{i-1,j}}{2h} \tag{2}$$

$$u_y\left(x_i, y_j\right) = \frac{u_{i,j+1} - u_{i,j-1}}{2h} \tag{3}$$

$$u_{xx}\left(x_i, y_j\right) = \frac{u_{i+1,j} - 2u_{i,j+}u_{i-1,j}}{h^2} \tag{4}$$

$$u_{yy}\left(x_i, y_j\right) = \frac{u_{i,j+1} - 2u_{i,j+}u_{i,j-1}}{h^2} \tag{5}$$

The Poisson equation can be approximated by using the above central difference quotients:

$$\frac{u_{i+1,j} - 2u_{i,j+}u_{i-1,j}}{h^2} + \frac{u_{i,j+1} - 2u_{i,j+}u_{i,j-1}}{h^2} = \mathrm{f}\left(x_i, y_j\right) \tag{6}$$

The boundary conditions of the boundary value problem need to be applied in accordance with the difference approximation of PDEs. The simplest of the boundary conditions is the Dirichlet boundary condition. In this case the difference equation can be applied to all interior points with unknown functions, and known values of the function at each boundary can be directly replaced.

Here, a simple type of Neumann boundary condition is taken into consideration. It is considered that boundary is taken at grid parallel to any of the axes here, e.g., x-axis. This boundary condition requires the normal derivative to be disappeared. This derivative in normal direction can be approximated by the central difference quotients.

$$\text{So, we approximate } \left.\frac{\partial u}{\partial n}\right|_{\mathrm{p}} = 0 \text{ as } \frac{u_{i+1,j} - u_{i-1,j}}{2h} = 0 \tag{7}$$

$$\text{which implies } u_{i+1,j} = u_{i-1,j} \tag{8}$$

The vanishing of normal derivative means that function $u(x,y)$ is symmetric about the boundary of the region.

2.2 Linear system solver

SOR is an iterative method, which is an important solver for the class of large linear system arising from the finite difference approximation of PDEs. It is not only an efficient solver but also a smoother. The method of relaxation is an iterative scheme which permits one to select the best equation to be used for the faster rate of convergence. Although Gauss Jacobi and Gauss Seidel are taken as one of the good iterative methods, relaxation method is more advantageous because of its faster rate of convergence depending upon the relaxation parameter 'ω.' When $0 < \omega < 1$, the procedures are called under relaxation methods. When ω = 1, then relaxation method is same as that of Gauss-Seidel method.

For $1 < \omega < 2$, the procedure is called over-relaxation.

The general Laplace equation is discretized by using finite differences, and the boundary conditions are approximated by second-order central differences. Fictitious points lying outside the domain, arising from the discretized form of derivative boundary conditions, are expressed in terms of the points and then incorporated into the governing finite difference equations. In order to have faster rate of convergence, the discretized form of Laplace equation in Eq. (9) can be approximated by using SOR method, which may take the form

$$u_{i,j}^{n+1} = u_{i,j}^{n} + \omega/4\left[\left(f\left(x_i, y_j\right) - 4u_{i,j}^{n} - a_{i+1,j}u_{i+1,j}^{n} - a_{i-1,j}u_{i-1,j}^{n+1} - a_{i,j+1}u_{i,j+1}^{n} - a_{i,j-1}u_{i,j-1}^{n+1}\right]\right. \tag{9}$$

where the value of relaxation factor 'ω' is obtained by hit and trial method in order to have faster rate of convergence.

The SOR iteration procedure can be terminated by using the following convergence criteria depending upon the convergence nature of the system being solved. In order to have computational results with a minimum number of iterations, absolute norm is used to decide the convergence criteria, which is given below:

$$e(i,j) = \left|\overline{u_{i,j}} - u_{i,j}\right| < \varepsilon \tag{10}$$

where ε is the order of convergence for each iteration and its value is taken as $\varepsilon = 0.00001$.

3. Problem formulation

In convective forced flow, the assumptions of negligible wall thickness and infinite conductivity of the fin and wall may cause unrealistic predictions of heat transfer characteristics, because of such ideal assumptions. In the present study, we take into account finite wall thickness of the inner pipe wall for realistic results. Also, we consider finite conductivity of the fin and wall in order to avoid the overestimates of heat transfer characteristics. This require coupling of the heat conduction problem in the wall-fin assembly and convective heat transfer problem in the fluid, and this coupled system is called conjugate heat transfer problem. The constant heat flux boundary condition is applied to the inner side of the inner pipe, and adiabatic thermal condition is applied at the inner wall of the outer pipe. At each solid-fluid interface, the heat flux is continuous. Moreover, temperature is assumed to be continuous.

In order to describe the conjugate problem mathematically, we need to describe the momentum, energy and heat equations that are to be solved simultaneously. The momentum and energy equations will be described in the prescribed sections and will be transformed into their dimensionless forms by the means of dimensionless variables. Similarly, heat equation is treated and solved for the transfer of heat in the solid part of the domain. A cross-sectional view of finned double pipe (FDP) is shown in **Figure 1**.

The velocity field is then independent of the temperature field. Geometrical symmetries shown in **Figure 1** permit the equations to be only solved in the region $a \le r \le b$ and $0 \le \theta \le \alpha + \beta$ shown in **Figure 2**.

3.1 Momentum, heat and energy equations

The governing momentum, heat and energy equations in dimensionless form are given in the Eqs. (11)–(13), as below by using the transformations defined in Syed [19].

This problem is constrained in the region where $r_i \le r \le r_o$ and $0 \le \theta \le \alpha + \beta$ because of its geometrical symmetry as shown in **Figure 2**:

$$\frac{\partial^2 u^*}{\partial R^2} + \frac{1}{R}\frac{\partial u^*}{\partial R} + \frac{1}{R^2}\frac{\partial^2 u^*}{\partial \theta^2} = \frac{4}{c} \tag{11}$$

where $C = -\left(1 - R_m^2 + 2R_m^2 \ln R_m\right)$

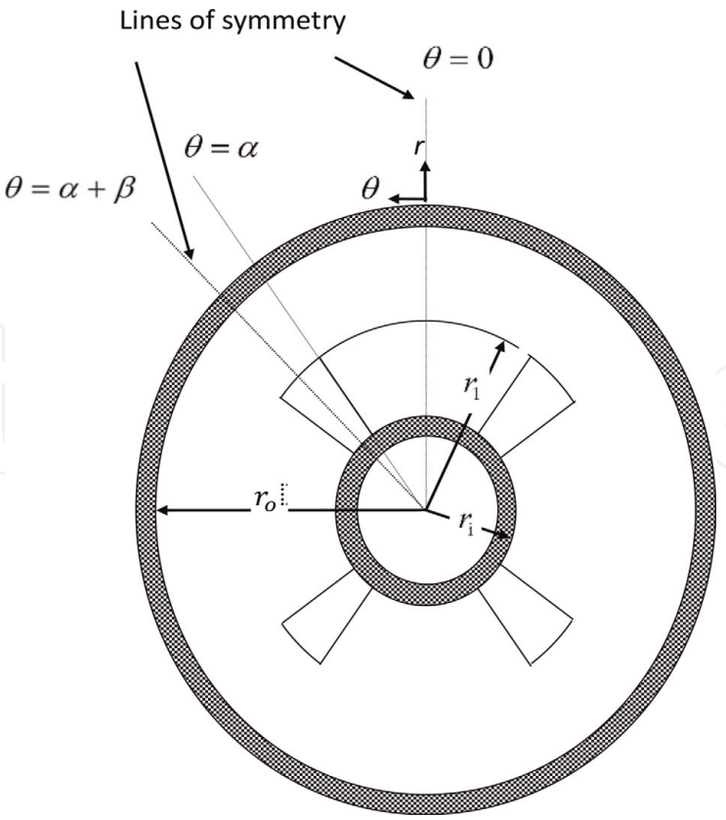

Figure 1.
Cross section of the finned double pipe.

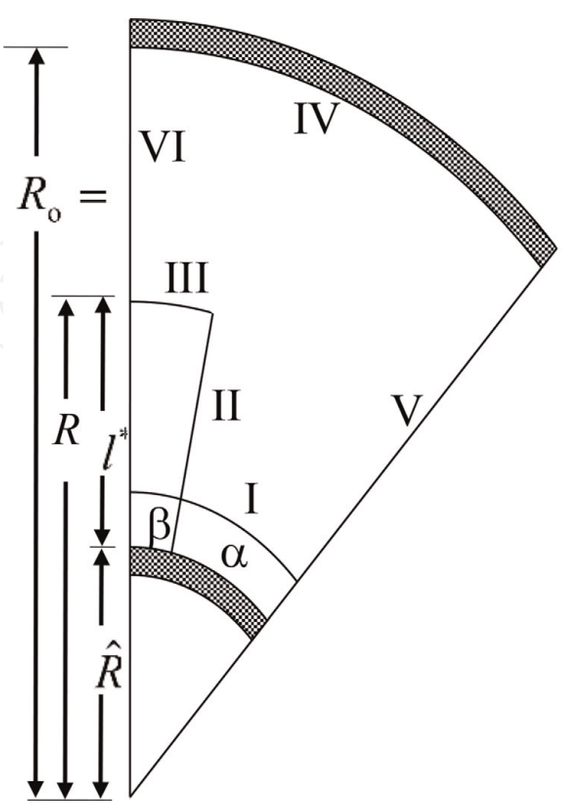

Figure 2.
Computational domain.

transformed into dimensionless form:

$$\frac{\partial^2 \tau^f}{\partial R^2} + \frac{1}{R}\frac{\partial \tau^f}{\partial R} + \frac{1}{R^2}\frac{\partial^2 \tau^f}{\partial \theta^2} = \frac{u^*}{A_c^* \overline{u}^*} \tag{12}$$

$$\frac{\partial^2 \tau^s}{\partial R^2} + \frac{1}{R}\frac{\partial \tau^s}{\partial R} + \frac{1}{R^2}\frac{\partial^2 \tau^s}{\partial \theta^2} = 0 \tag{13}$$

where $\overline{u}^*$ is the dimensionless mean velocity.

The boundary conditions are applied due to the viscosity of the fluid and symmetry offered by the domain shown in **Figure 2**. The boundary conditions in dimensionless form may be written as:

a. No slip conditions at the solid boundaries:

$$\text{(I)}\ u^* = 0 \text{ at } R = \hat{R},\ 0 \le \theta \le \alpha$$
$$\text{(II)}\ u^* = 0 \text{ at } \theta = \alpha,\ \hat{R} \le R \le R_1$$
$$\text{(III)}\ u^* = 0 \text{ at } R = R_1,\ \alpha \le \theta \le \alpha + \beta$$
$$\text{(IV)}\ u^* = 0 \text{ at } R = 1,\ 0 \le \theta \le \alpha + \beta$$

b. Symmetry conditions:

$$\text{(V)}\ {}^{\partial u^*}/_{\partial \theta} = 0 \text{ at } \theta = 0,\ \hat{R} \le R \le R_1$$
$$\text{(VI)}\ {}^{\partial u^*}/_{\partial \theta} = 0 \text{ at } \theta = \alpha + \beta,\ R_1 \le R \le 1$$

Constant flux boundary condition at the inner surface of the inner pipe

$$\tau = 0 \text{ at R} = R_w,\ 0 \le \theta \le \alpha \tag{14}$$

An adiabatic wall temperature condition at the inner surface of the outer pipe

$$\frac{\partial \tau}{\partial \theta} = 0 \text{ at R} = 1,\ 0 \le \theta \le \alpha + \beta \tag{15}$$

Boundary conditions at the lines of symmetry

$$\frac{\partial \tau^s}{\partial \theta} = 0 \text{ at } \theta = 0,\ R_w \le R \le R_o \tag{16}$$

$$\frac{\partial \tau^f}{\partial \theta} = 0 \text{ at } \theta = 0,\ \hat{R} \le R \le 1 \tag{17}$$

$$\frac{\partial \tau^s}{\partial \theta} = 0 \text{ at } \theta = \alpha + \beta,\ R_w \le R \le R_1 \tag{18}$$

$$\frac{\partial \tau^f}{\partial \theta} = 0 \text{ at } \theta = \alpha + \beta,\ \hat{R} \le R \le 1 \tag{19}$$

There are three interfaces where the solid and fluid mediums are contact. These three interfaces are termed here as inner pipe, fin lateral surface and fin tip interfaces. These may be defined as

$$\text{Inner pipe interface is at } r = r_i \& 0 \le \theta \le \alpha. \tag{20}$$

$$\text{Fin lateral surface interface is at } \theta = \alpha \& r_i \le r \le r_1 \tag{21}$$

$$\text{Fin tip interface is at } r = r_1 \text{ and } \alpha \le \theta \le \alpha + \beta. \tag{22}$$

On these interfaces, we impose the conditions of continuity of temperature and that of heat flux in order to maintain the energy balance. These interface conditions are used to couple conduction (Eq. (13)) in the solid with the energy (Eq. (12)) in the fluid. This forms the so-called conjugate problem.

The interface conditions can be expressed mathematically as given below by using same dimensionless transformations.

Continuity of fluxes at the solid-fluid interfaces

$$\frac{\partial \tau^s}{\partial R} = \frac{1}{\Omega}\frac{\partial \tau^f}{\partial R} \text{ at } R = \hat{R} \text{ and } 0 \le \theta \le \alpha \tag{23}$$

$$\frac{\partial \tau^s}{\partial R} = \frac{1}{\Omega}\frac{\partial \tau^f}{\partial R} \text{ at } R = R_1 \text{ and } \alpha \le \theta \le \alpha + \beta \tag{24}$$

$$\frac{\partial \tau^s}{\partial \theta} = \frac{1}{\Omega}\frac{\partial \tau^f}{\partial \theta} \text{ at } \theta = \alpha \text{ and } \hat{R} \le R \le R_1 \tag{25}$$

where $\Omega = \frac{\lambda^f}{\lambda^s}$ is the ratio of conductivities of fluid by solid.

Continuity of temperature at the solid-fluid interfaces

$$\tau^s = \tau^f \text{ at } R = \hat{R} \text{ and } 0 \le \theta \le \alpha \tag{26}$$

$$\tau^s = \tau^f \text{ at} R = R_1 \text{ and } \alpha \le \theta \le \alpha + \beta \tag{27}$$

$$T^s = T^f \text{ at } \theta = \alpha \text{ and } \hat{R} \le R \le R_1 \tag{28}$$

3.2 Numerical solutions

For numerical domain, Poisson equation given in Eq. (1) takes the form

$$\frac{U_{i+1,j} - 2U_{i,j} + U_{i-1,j}}{h^2} + \frac{1}{R_i}\frac{U_{i+1,j} - U_{i-1,j}}{2h} + \frac{1}{R_i^2}\frac{U_{i+1,j} - 2U_{i,j} + U_{i-1,j}}{k^2} = \frac{4}{C} \tag{29}$$

After combining the coefficient, we get

$$\left(\frac{1}{h^2} + \frac{1}{2R_i h}\right)U_{i+1,j} + \left(\frac{-2}{h^2} - \frac{2}{R_i^2 k^2}\right)U_{i,j} + \left(\frac{1}{h^2} - \frac{1}{2R_i h}\right)U_{i-1,j} + \frac{1}{R_i^2 k^2}U_{i,j+1} + \frac{1}{R_i^2 k^2}U_{i,j-1} = \frac{4}{C} \tag{30}$$

For our simplicity, writing the coefficient in some standardized form

$$\mathrm{eU_{i+1,j}} + \mathrm{pU_{i,j}} + \mathrm{wU_{i-1,j}} + \mathrm{nU_{i,j+1}} + \mathrm{sU_{i,j-1}} = \mathrm{rhs}$$

$$\text{where } e = \left(\frac{1}{h^2} + \frac{1}{2R_i h}\right), p = \left(\frac{-2}{h^2} - \frac{2}{R_i^2 k^2}\right),$$

$$\mathrm{w} = \left(\frac{1}{\mathrm{h}^2} - \frac{1}{2\mathrm{R_i h}}\right), \mathrm{n} = \frac{1}{\mathrm{R_i^2 k^2}}, \mathrm{s} = \frac{1}{\mathrm{R_i^2 k^2}}, \mathrm{rhs} = \frac{4}{\mathrm{C}}$$

For energy and heat equations, similar scheme is developed.

3.3 Error analysis and validity of results

The numerical algorithm described in Chapter 2 has been used to determine the numerical results in the present study. The iterative convergence and interpolation

procedure need to be validated. The error criterion given as $\varepsilon = 0.00001$ was used to terminate the iterative procedures. The present results of the friction factor and Nusselt number for copper have been compared with literature results for β = 3°. They were verified by comparing them with results present in literature with same geometrical parameters of heat exchanger. The present results differ with the literature results by less than 0.5%. However, in two exceptional cases, the results are not up to the same level of accuracy. The improved results obtained at all grid levels are of comparable accuracy. The comparison given in **Table 1** confirms the validity of numerical algorithm. This difference between friction factor and Nusselt number gives the overview; the percentage difference greater than '0' depicts the overestimation in present results, and difference less than '0' shows the underestimated values of the present study. Since the difference in the values provided in **Table 1** is negligible, this gives the validity of results in the present study.

4. Result and discussion

4.1 Local results

4.1.1 Flow behaviour

In this section, velocity contours are given with respect to different geometrical variations. **Figure 3a** and **b** show the velocity contours for $\hat{R} = 0.5$, $\beta = 2^{o}$, H^{*} = 0.6. The effect of the number of fins is observed by firstly taking *M = 6* and then *M = 18.*

While observing the contours, it is clear that between two consecutive fins a region of high velocity exists in the middle of annulus.

4.1.1.1 Velocity contours

Figure 3a shows the velocity contours, For *M=6,* the annulus region is filled with closed loops in the middle of the region, while near the inner wall of outer pipe circular loops are formed. For this fin height, two dimensional effects are more towards the outer pipe.

Figure 3b shows the velocity contours for *M = 18*, for H^{*} = 0.6. For the increased number of fins, the middle of region is surrounded by annular loops, which depict

Geometrical parameters		Comparison of friction factor			Comparison of Nusselt number		
M	H^{*}	f**Re**	f**Re**	**Age change (%)**	**Nu(Old)**	**Nu(Cu)**	**Age change (%)**
6	0.2	21.117	21.1351	0.0857	4.5189	4.5212	0.0508
	0.4	20.401	20.4185	0.0857	4.1846	4.1881	0.0836
	0.6	18.848	18.8592	0.0594	3.9827	3.9873	0.1154
	0.8	15.783	15.7868	0.0240	3.766	3.3789	−10.278
12	0.2	19.125	19.1580	0.1725	3.8433	3.4873	−9.262
	0.4	19.358	19.3991	0.2123	3.1644	3.1705	0.1928
	0.6	20.027	20.0653	0.1912	3.9256	3.9421	0.4203
	0.8	17.145	17.1592	0.0828	4.2311	4.2401	0.2127

Table 1.
Validity of present results of momentum equation and energy equation for $\beta = 3°$, $\hat{R} = 0.5$.

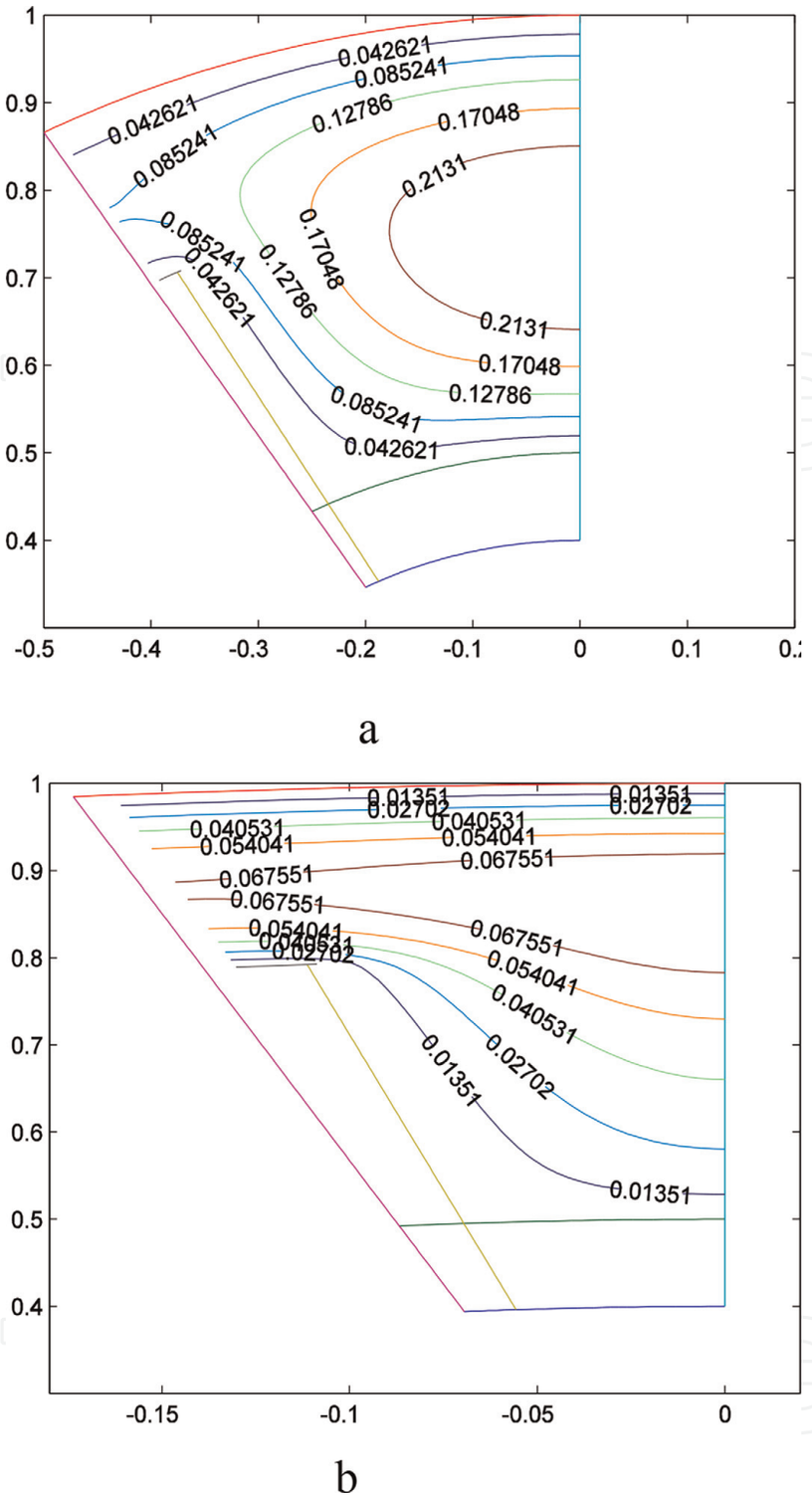

Figure 3.
(a) Velocity contours for $\hat{R}$ = 0.5, H^* = 0.8, M = 6. (b) Velocity contours for $\hat{R}$ = 0.5, H^* = 0.8, M = 6.

that the region of high velocity starts to develop at the middle of annulus. Also, when a number of fins are increased, then closed loop will break into annular loops.

We must have to notice that increase in the number of fins will also give rise to the value of friction factor, which may slow down the fluid motion in the pipe.

4.1.2 Heat transfer analysis

The results of energy and heat equations are combined together for analytical study of conjugate heat transfer, while fin and wall are offering finite heat conduction because of material used in them.

The same geometrical parameters and grid points are taken as that for momentum equation. A comparative study on behaviour of heat transfer is shown in **Figure 4a** and **b**. While using copper for fin and wall geometry, it should be noted that the isotherms corresponding to the zero level represent the geometry. Because of the definition of the dimensionless temperature used, the higher the isotherm level depicts, the lower the value of local temperature. The isotherms corresponding to value 1 have local fluid temperature equal to mean fluid temperature. Those with values lower than 1 have the local temperature greater than the mean temperature, and while greater than 1 indicate that the local temperature is lesser than the meant temperature. From these figures, it is clear that the region of high-temperature gradient near the inner pipe wall and near fin surface shows the high rate of convection. In order to comprise with interfaces and transfer of heat between fluid and solid, continuity of fluxes and of temperature is considered.

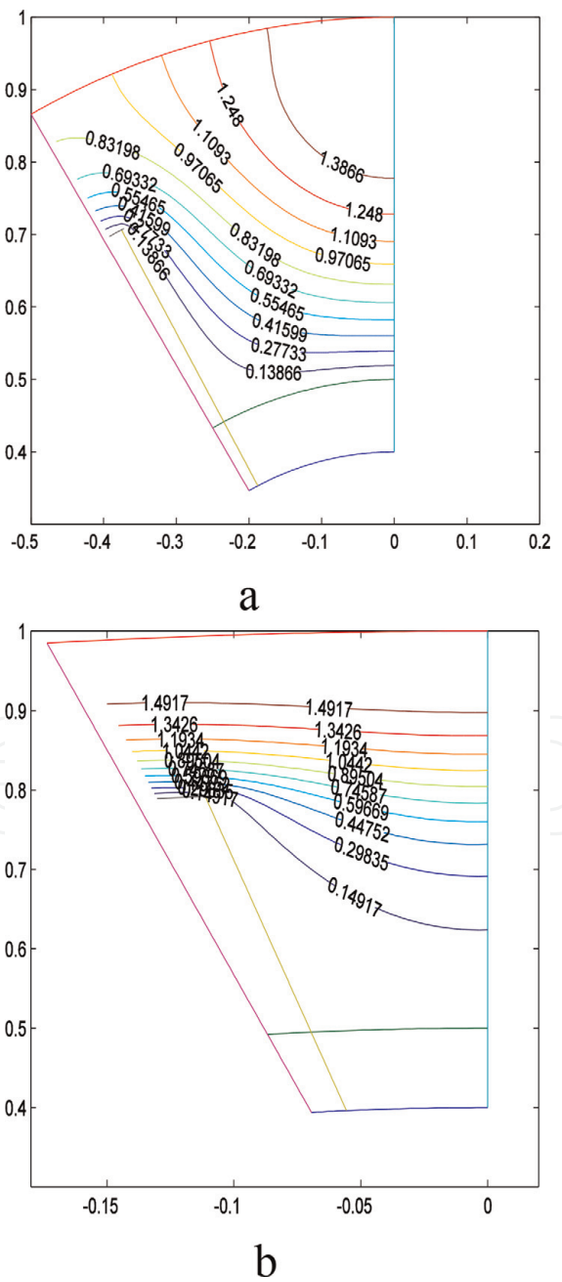

Figure 4.
(a) Isotherms (copper) for $\hat{R}$ = 0.5, H^* = 0.6, M = 6. (b) Isotherms (copper) for $\hat{R}$ = 0.5, H^* = 0.6, M = 18.

4.1.2.1 Isotherms

Figure 4a shows the isotherms for $M = 6$, $\hat{R} = 0.5$, $H^* = 0.6$, which shows that a region of higher temperature starts to develop in the middle of annulus and significant change occurs in temperature gradient. Whereas, **Figure 4b** shows the isotherms, when $M = 18$, the temperature gradient is higher in the entire cross section, and higher temperature region appears near the outer wall of the inner pipe, while lower near the inner wall of the outer pipe.

Apparently, in these isotherms conduction in wall and fin assembly is not being shown, but if we increase the number of contours, the temperature gradient is shown in the solid part of the domain too. This is because of the very high-temperature gradient in fluid and because of convection and conduction.

The trend of isotherms is more understandable corresponding to the velocity contours. From these figures, it is observed that the region of high-velocity gradients near the heated surfaces of the inner pipe and fin also has high-temperature gradients indicating the high rate of convection.

There is an equivalent transfer of heat in fin and fluid on the interfaces; interfaces get smoother because of the continuity of fluxes. But in case of temperature difference, it rises more rapidly in fluid than the solid (wall and fin).

4.2 Overall results

Figure 5a shows the plots of different values of Nusselt number of copper against the number of fins $H^* \in \{0.2, 0.4, 0.6, 0.8\}$ taking fixed value of ratio of radii $\hat{R} = 0.5$. For fin height $M = 6$, the value of Nusselt number decreases as we increase fin height. The plot of Nusselt number against these values shows monotonic decreasing behaviour. However, the value of Nu(Cu) remains higher for the $H^* = 0.2$ than the fin height $H^* = 0.4$ and others.

The plots of Nusselt numbers for $M = 6$ and $M = 18$ clearly depict that the behaviour of Nusselt number significantly differs in these two graphs. An optimal value of Nusselt number is observed for some particular value of $H^* = 0.2$ used. Thus, for $M = 6$, shorter fin gives better rate of heat conduction.

While taking the higher number of fins into account, for $M = 18$, Nusselt number gradually decreases when fin height is increased from $H^* = 0.2$ to $H^* = 0.4$. Its shows a parabolic behaviour. After reaching its lowest value, it starts increasing and attains its optimal value at the longest fin.

It can be concluded that the value of Nusselt number for $\hat{R} = 0.5$ at $H^* = 0.6$ and $H^* = 0.8$ is the best choice when $M = 9$ and $M = 18$ are taken, respectively.

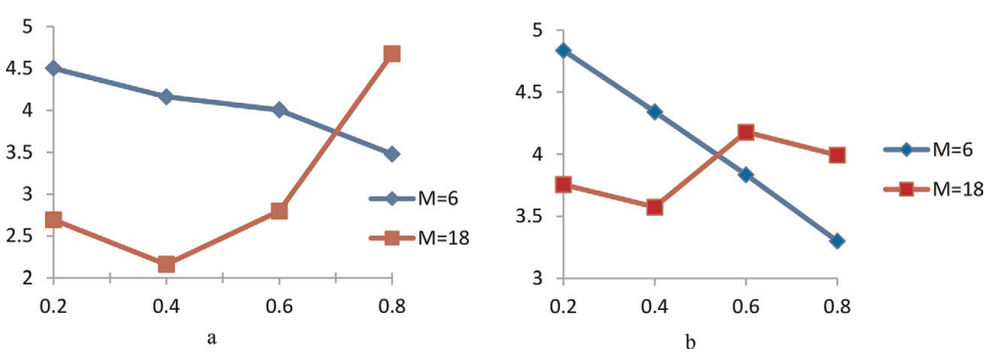

Figure 5.
(a) H-Nu(Cu), for $\hat{R} = 0.5$. (b) M-Nu(Cu), for $\hat{R} = 0.7$.*

Figure 5b shows the plots of different values of Nusslet number of copper against number of fins $H^* \in \{0.2, 0.4, 0.6, 0.8\}$ taking fixed value of ratio of radii $\hat{R} = 0.7$.

For $\hat{\boldsymbol{R}} = \mathbf{0.7}$, $M = 6$, heat transfer coefficient shows monotonic decreasing behaviour as we increase fin height. For $H^* = 0.2$, the value is Nusselt number is highest.

While for the increased number of fins, $M = 18$, Nusselt number shows alternating behaviour for different values of fin height. It firstly decreases and then it starts increasing. For $H^* = 0.6$, it gives its largest value.

From the above two comparisons, we can deduce that for the less number of fins, if we increase the fin height, it reduces the increase in heat transfer. While for more number of fins, longer fins give more optimal results.

5. Conclusion

The results presented in previous sections can be concluded as follows:

- A comparison of present results with the literature results gives the validity proof of the numerical study.
- The number of fin and fin heights are most effective geometrical parameters.
- The influences of geometrical parameters are dependent on each other.
- The location of the regions of high velocities is dependent on geometrical parameters.
- Large velocity gradients exist near the fin tip and outer pipe inner surfaces.
- The value of $\hat{R}$ affects the heat transfer rate significantly, for larger fins and for higher number of fins.
- The value of Nusselt number at $M = 18$, $\hat{R} = 0.5$, gives the optimal value for $H^* = 0.8$.
- For $\hat{R} = 0.7$, the value of Nu(Cu) goes on increasing with higher values of M, at $H^* = 0.8$.

Author details

Ghazala Ashraf[1]*, Khalid S. Syed[2] and Muhammad Ishaq[1]

1 Department of Mathematics, COMSATS University Islamabad, Vehari Campus, Pakistan

2 Centre for Advanced Studies in Pure and Applied Mathematics, Bahauddin Zakariya University, Multan, Pakistan

*Address all correspondence to: ghazalaashraf@ciitvehari.edu.pk

References

[1] Incropera FP, DeWitt DP. Fundamentals of Heat and Mass Transfer. 4th ed. New York: John Wiley and Sons; 1996

[2] Özisik MN. Heat Transfer-a Basic Approach. McGraw-Hill Book Company; 1985

[3] Nasiruddin MH, Siddiqui K. Heat transfer augmentation in a heat exchanger tube using a baffle. International Journal of Heat and Fluid Flow. 2007;**28**:318-328

[4] Zeitoun O, Hegazy AS. Heat transfer for laminar flow in internally finned pipes with different fin heights and uniform wall temperature. Heat and Mass Transfer. 2004;**40**:253-259

[5] Suryanarayana NV, Apparao TVVR. Heat transfer augmentation and pumping power in double-pipe heat exchangers. 1994;**9**(4):436-444

[6] Li Q, Ma L, Chen Z, Warnecke H-J. Heat transfer characteristics of tube with elliptic pin fins in cross flow of air. Heat and Mass Transfer. 2003;**39**: 529-533

[7] Adegun IK, EL-Suleiman A, Hussein AK. Numerical simulation of forced convective flow and heat transferrin gravitational inclined circular pipes with equi-spaced internal fins. Journal of Basic and Applied Scientific Research. 2013;**3**(10):182-193

[8] Pagliarini G. Effects of axial conduction in the wall and the fluid on the conjugate heat transfer in thick-walled circular tubes. International Communications in Heat and Mass Transfer. 1988;**15**:581-591

[9] Dorfman A, Renner Z. Conjugate problems in convective heat transfer. Mathematical Problems in Engineering. 2009;**27**

[10] Kumar IO. Conjugate problems of heat transfer in laminar boundary layer with injection. Journal of Engineering Physics. 1968;**14**(5):411-416

[11] Barozzi GS, Pagliarani G. A method to solve conjugate heat transfer problems: The case of fully developed laminar flow in a pipe. Journal of Heat Transfer. 1985;**107**:77-83

[12] Mori S, Sakakibara M, Tanimoto A. Steady heat transfer to laminar flow with conduction in the wall tube. Heat Transfer Japanese Research. 1976;**5**(4): 17-25

[13] Sakakibara M, Mori S, Tanimoto A. Conjugate heat transfer with laminar flow in an annulus. The Canadian Journal of Chemical Engineering. 1987; **65**:541-549

[14] Kettner IJ, Degani D, Gutfinger C. Numerical study of laminar heat transfer in internally finned tubes. Numerical Heat Transfer, Part A. 1991; **20**:159-180

[15] Fiebig M, Grosse-Gorgemann A, Chen Y, Mitra NK. Conjugate heat transfer of a finned tube. Part A: Heat transfer behaviour and occurrence of heat transfer reversal. Numerical Heat Transfer, Part A. 1995;**28**:133-146

[16] Nguyen TM, Khodadadi JM, Vlachos NS. Laminar flow and conjugate heat transfer in rib roughened tubes. Numerical Heat Transfer, Part A. 1989; **15**:165-179

[17] Nordstorm J, Berg J. Conjugate heat transfer using modified interface conditions for Navier-Stokes equations. LiTH-MAT-R–2011/18–SE

[18] Sohail M, Fakhir Hasani HS. Conjugate conduction—Convection of finned tube annulus in longitudinal

laminar flow. In: Proceedings of the 4th BSME-ASME International Conference on Thermal Engineering; 27–29 December, 2008

[19] Syed KS, Iqbal M, Mir NA. Convective heat transfer in the thermal entrance region of finned double-pipe. Heat and Mass Transfer. 2007;**43**: 449-457

[20] Iqbal M. Numerical study of laminar heat transfer through a finned double-pipe heat exchanger [PhD thesis]. Multan, Pakistan: Centre for Advanced Studies in Pure and Applied Mathematics (CASPAM), Bahauddin Zakariya University; 2006